High-resolution climate variability across the Piacenzian/Gelasian boundary in the Monte San Nicola section (Sicily, Italy)

Elena Zanola [a,*], Sergio Bonomo [b], Alessandro Incarbona [c], Agata Di Stefano [d], Salvatore Distefano [d], Patrizia Ferretti [e], Eliana Fornaciari [a], Simone Galeotti [f], Patrizia Macrì [g], Isabella Raffi [h], Nadia Sabatino [i], Fabio Speranza [g], Mario Sprovieri [j], Enrico Di Stefano [c], Rodolfo Sprovieri [f], Domenico Rio [a], Luca Capraro [a]

[a] Dipartimento di Geoscienze, Università degli Studi di Padova, Via G. Gradenigo 6, 35131, Padova, Italy
[b] CNR- Istituto di Geologia Ambientale e Geoingegneria (IGAG), Area Della Ricerca di Roma, 1 – Strada Provinciale 35d, 9-00010, Montelibretti, Italy
[c] Dipartimento di Scienze della Terra e del Mare, Via Archirafi 22, 90123, Palermo, Italy
[d] Dipartimento di Scienze Biologiche, Geologiche e Ambientali, Università degli Studi di Catania, Corso Italia 57, 95100, Catania, Italy
[e] Dipartimento di Scienze Ambientali, Informatica e Statistica, Università Ca' Foscari di Venezia, Via Torino 155, 30172, Venezia, Italy
[f] Dipartimento di Scienze Pure e Applicate, Università degli Studi di Urbino, Via Ca' Le Suore 2-4, 61029, Urbino, Italy
[g] Istituto Nazionale di Geofisica e Vulcanologia (INGV), Via di Vigna Murata 605, 00143, Roma, Italy
[h] International Research School of Planetology - IRSPS, Università degli Studi "G. D'Annunzio" di Chieti-Pescara, Viale Pindaro, 42, 65127, Pescara, Italy
[i] Istituto per lo studio degli impatti Antropici e Sostenibilità in ambiente marino (IAS-CNR), Palermo (ex Complesso Roosevelt, Lungomare Cristoforo Colombo, 4521, 90149, Loc. Addaura), Italy
[j] Istituto di Scienze Marine (ISMAR-CNR), Venezia (Tesa 104 – Arsenale, Castello 2737/F 30122), Italy

ARTICLE INFO

ABSTRACT

The Piacenzian – Gelasian transition is a time of profound changes in the Earth's climatic regime, epitomized by the definitive establishment of large ice caps in the Northern Hemisphere and the beginning of the "ice ages" at ca. 2.6 Ma. This event is sharply documented in $\delta^{18}O$ records globally by a prominent triplet of severe glacial events (MIS 100, 98 and 96) that approximate the base of the Gelasian Stage. We have reconstructed a multi-species planktic and benthic foraminiferal $\delta^{18}O$ and $\delta^{13}C$ record from the Monte San Nicola section (Sicily) across the Piacenzian/Gelasian boundary, with the purpose of better constraining in time the main marker criteria for recognition of the Gelasian GSSP (Global Boundary Stratotype Section and Point) and investigating in detail the paleoclimatic and paleoceanographic response of the central Mediterranean to the definitive onset of the Northern Hemisphere Glaciation. Our results confirm the reliability and usability of the criteria originally proposed for defining the Gelasian GSSP, and significantly improve their chronology and chronostratigraphic positioning. Beyond an obvious alternation of obliquity-driven glacial-interglacial cycles, our isotopic record unraveled a pervasive climate variability in the suborbital time domain, the origin of which is still ambiguous. Altogether data presented in this paper provide the first high resolution isotopic records shedding new light both on the stratigraphic and paleoclimatic evolution of the Central Mediterranean area at the beginning of the Northern Hemisphere Glaciation.

1. Introduction

The Quaternary System underwent a profound revision, after its formal subdivision into Subseries, the ratification of the Lower/Middle Pleistocene boundary and, most importantly, the lowering of the Pliocene/Pleistocene boundary to the base of the Gelasian Stage (ca. 2.588 Ma) (Gibbard et al., 2010; Head et al., 2021). The Gelasian, originally

defined as the third (Upper) Stage of the Pliocene Series above the Piacenzian (Rio et al., 1998), currently serves as the basal chronostratigraphic unit of both the Pleistocene Series and the Quaternary System (Gibbard et al., 2010). In the wake of these changes, the scientific relevance of the events around the Piacenzian/Gelasian boundary is growing fast, and the previously overlooked Monte San Nicola section (southern Sicily), where the Gelasian GSSP is located, is becoming even

more notorious within the Quaternary scholarly community.

The Piacenzian–Gelasian transition marks the switch from "Coolhouse" to "Icehouse" climate states (Westerhold et al., 2020), a key event in the climatic evolution of the Cenozoic. Specifically, the "warm" (>2–3 °C than pre-industrial) mid-Piacenzian interval (ca. 3.3–3.1 Ma) (McClymont et al., 2020; Seki et al., 2010) was followed by a phase of intensifying Northern Hemisphere Glaciation that, beginning from glacial Marine Isotopic Stage (MIS) 100, culminated with the definitive establishment of large Northern Hemisphere Ice Sheets and the periodic deposition of ice-rafted detritus (IRD) in the North Atlantic (Jakob et al., 2020; Rohling et al., 2014). Not by chance, MIS 100 is traditionally recognized as marker of the "beginning of the ice ages" (Shackleton et al., 1984). Long-term changes in the strength of the Atlantic Meridional Overturning Circulation (AMOC) and the closure of the Central American Seaway have been proposed as the main drivers of this climatic breakthrough (Bartoli et al., 2005; Hayashi et al., 2020a,b). Nonetheless, the underlying mechanisms and regional responses to this event in the Mediterranean area are still debated and poorly documented, in spite of the rich stratigraphic record straddling the interval of relevance and the plenty of information found within (e.g., Zijderveld et al., 1991; Pasini and Colalongo, 1997; Capraro et al., 2011).

The present work is aimed at characterizing the paleoclimatic and paleoceanographic evolution of the central Mediterranean in the interval across the Piacenzian/Gelasian (current Pliocene/Pleistocene) boundary. In addition, it is intended to yield refined information on the chronostratigraphic position and age of key markers of the Gelasian GSSP in its type-area (Rio et al., 1998). Namely, these are the "Nicola bed" (i.e. MPRS A5, i-cycle 250; Fig. 1), a prominent sapropel layer that provides physical reference for the Piacenzian/Gelasian boundary (Verhallen, 1987; Zijderveld et al., 1991; Hilgen, 1991); the Gauss/-Matuyama geomagnetic reversal, which closely approximate the base of the Gelasian Stage (Channell et al., 1992); the Top of calcareous nannofossils *Discoaster pentaradiatus*, representing the most convenient event for the biostratigraphic correlation of the boundary (Raffi et al., 2006; Rio et al., 1994).

2. Material

The study area is in the western sector of Monte San Nicola badlands, ca. 10 km north of Gela, Southern Sicily (Italy; Fig. 1a). The local stratigraphy consists in a stack of deep-marine, cyclically organized muds that contain four sapropel clusters (O, A, B, C; Verhallen, 1987; Zijderveld et al., 1991), the uppermost sapropel of cluster A (MPRS A5, the notorious "Nicola bed") being the lithological marker of Gelasian GSSP (Rio et al., 1998). We focused our investigation on the lower part of the "Mandorlo" section of Capraro et al. (2022), which is characterized by a better exposure, ease of access and stratigraphic continuity with respect to the historical "Type" section of Channell et al. (1992), where the Gelasian GSSP has been defined (Rio et al., 1998). As previously demonstrated by Becker et al. (2005) for the MIS 100 interval in a stratigraphic profile close to the Mandorlo section, the succession of relevance is perfectly suited for high-resolution paleoclimatic and paleoceanographic studies.

We reconstructed a low-resolution isotopic record for *C. pachyderma* and *G. ruber* in the interval between −745 cm (slightly above sapropel A1) and +475 cm (lower part of the gray clayey band separating sapropel clusters A and B) using the samples presented in Capraro et al. (2022), which were collected every 33 cm. The high-resolution isotopic record for *Uvigerina* spp was obtained from a set of 200 samples, collected along the very same profile every 5 cm, in the interval between −300 cm (= top of sapropel A4) and +700 cm (= just above the dark clayey layer associated to i-cycle 242). For the sake of consistency, the top of the Nicola bed was established as the stratigraphic reference (zero) level for both records. Prominent physical stratigraphic markers above and below the boundary ensure correlation between the datasets, which however proved to overlap almost perfectly with no need for

further calibration.

3. Methods

3.1. Stable isotopes

Stable isotope analyses for *G. ruber* and *C. pachyderma* were carried out on 30 and 27 samples, respectively (Fig. 2; Table 1). For *Uvigerina* spp, 193 data points have been generated out of the 200 investigated samples, because 7 specimens from within sapropel A5 were barren of suitable benthic meiofauna.

Regarding *Uvigerina* spp, 15 specimens per sample were treated before the isotopic analysis according to the classical foraminiferal tests cleaning protocol (Shackleton et al., 1995). Foraminifer tests were gently crushed in glass vials, soaked in H_2O_2 (3%) for 30 min, soaked in acetone within an ultrasound bath for 30 s, and finally dried in oven at 50 °C for 12 h. Measurements were carried out at the mass spectrometer laboratory of the Department of Geosciences of the University of Padova by means of a Thermo Scientific Delta V Advantage mass spectrometer linked to an automated continuous flow Gas Bench II. Samples acidification was performed at 70 °C. An internal standard for quality control (marble from the contact aureola of the Monzoni intrusive complex, the Dolomites, with $\delta^{18}O = -10.44$ and $\delta^{13}C = 0.68$) was measured every ca. 30 samples; a second standard for calibration (Carrara marble with $\delta^{18}O = -1.15$ and $\delta^{13}C = 2.58$) was measured at least every 7 samples. The isotopic composition of the standards is periodically tested against international standards. The external error, derived by repeated measures of the quality control standard, is better than 0.05 ‰ and better than 0.10 ‰, respectively for $\delta^{13}C$ and $\delta^{18}O$. All the isotopic data are given as per mil (‰) relative to the VPDB standard.

Analyses for *G. ruber* and *C. pachyderma* (10–15 foraminifer tests per species/sample) were performed at the IAS-CNR (Capo Granitola) isotope geochemistry laboratory by means of a ThermoElectron Delta V mass spectrometer coupled to an automated continuous flow carbonate preparation GasBenchII device (Spötl and Vennemann, 2003). Samples acidification was performed at 50 °C. An internal standard (Carrara Marble with $\delta^{18}O = -2.43$ vs. VPDB and $\delta^{13}C = 2.43$ vs. VPDB) was run every 6 samples. Given the small number of samples, a sample of NBS19 international standard was only measured at the beginning of the analysis. Standard deviations of carbon and oxygen isotope measures were estimated at 0.06 and 0.1 ‰, respectively. All isotope data are reported in per mil (‰) relative to the VPDB standard.

3.2. Spectral analysis

The analysis of non-stationary (frequency changes with time) and non-linear signals was performed by applying the Ensemble Empirical Mode Decomposition algorithm (EEMD) by (Wu and Huang, 2009). The EEMD is an adaptive noise-assisted data analysis method that improves the ordinary Empirical Mode Decomposition (EMD) by (Huang et al., 1998). Decomposition provides a powerful method to investigate the different processes behind a given time series data and separates short time-scale events from a general trend. This technique is based on the assumption that any complicated signal can be decomposed into a finite, often small, number of components defined as "Intrinsic Mode Functions" (IMFs) (Huang et al., 1998). Each IMF represents an embedded characteristic simple oscillation on a separated timescale. IMF components were analyzed with "REDFIT" and Wavelet transform (WT). All data were detrended prior to running the spectral analysis, subtracting a linear regression line from the analyzed data. All analyses were carried out with R (version 4.1.3) using the Rlibeemd (Luukko et al., 2016), dplR (Bunn, 2010), and Biwavelet (Liu et al., 2007) packages.
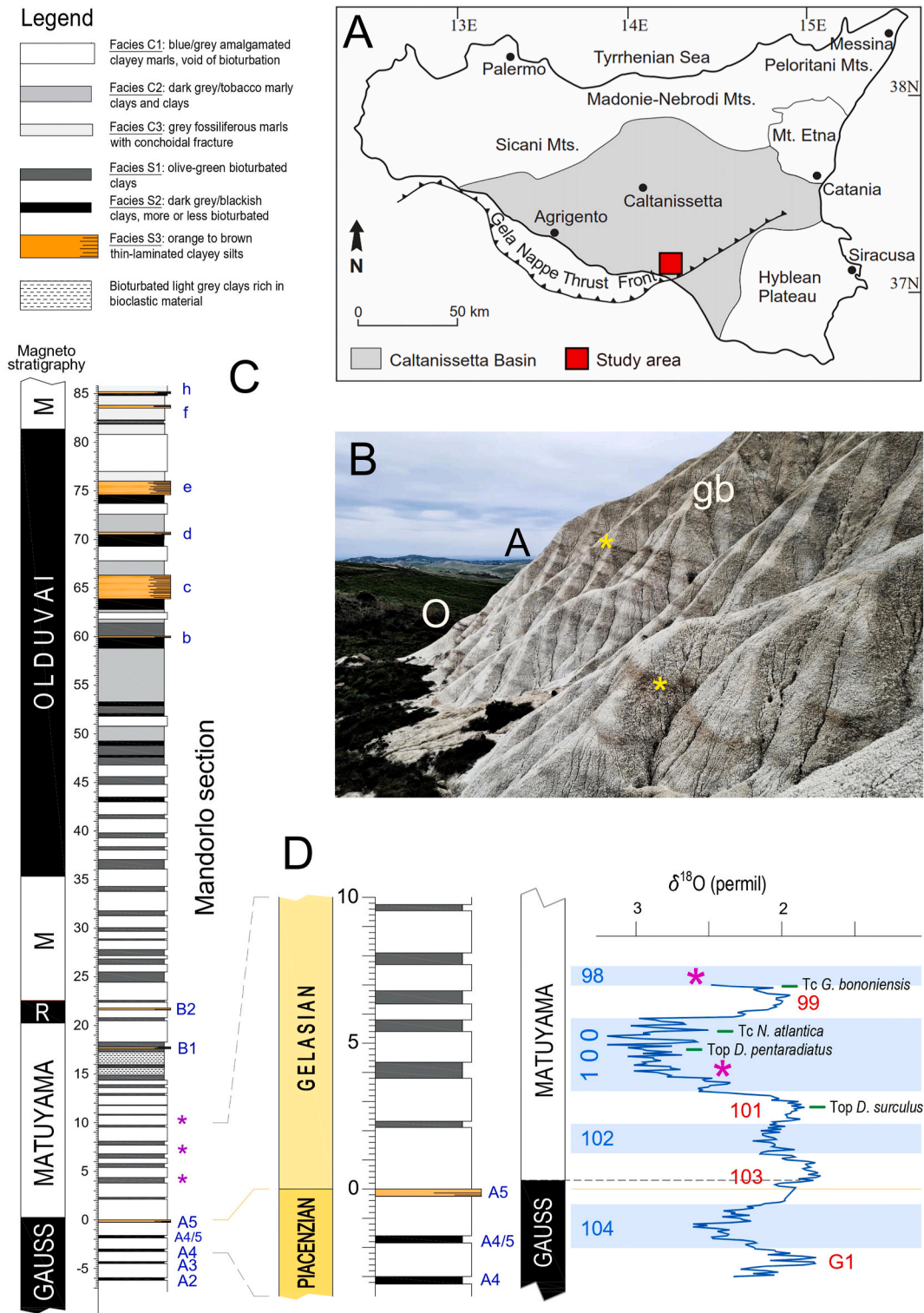
Fig. 1. A) Position of the Monte San Nicola area (red box) within the Caltanissetta sedimentary Basin (Sicily). B) Sapropel clusters O and A (upper Piacenzian) in the badlands close to the Mandorlo section. Yellow asterisks indicate the "Nicola bed" (sapropel A5), physical reference for the Piacenzian/Gelasian boundary. The tripartite gray band (gb in figure) at the change of slope above the "Nicola bed" contains the MIS 100 – MIS 96 interval. C) Essential stratigraphic information for the Mandorlo section (modified from Capraro et al., 2022). Left: magnetostratigraphy of section. R: Reunion; M: Matuyama. Right: lithological log; legend is reported above. Individual sapropel layers of clusters A, B and C are labeled in blue. Purple stars: episodic influxes of left-coiled *Neogloboquadrina atlantica*, deemed as correlative to MIS 100, 98 and 96 (see Becker et al., 2005). D) Blow-up of the stratigraphic interval of relevance for this study. Left: chronostratigraphic, lithological, and magnetostratigraphic logs (same as above). Right: the δ18O record for *Uvigerina* spp, with indication of glacial (blue) and interglacial (red) MISs. Light blue bands indicate glacial intervals. Purple stars as above. Green lines: stratigraphic position of the biohorizons identified within the interval of relevance (see Capraro et al., 2022). Tc: Top common. The thin orange line marks the Piacenzian/Gelasian boundary. The dashed line indicates the position of the Gauss/Matuyama geomagnetic reversal as defined by Capraro et al. (2022).
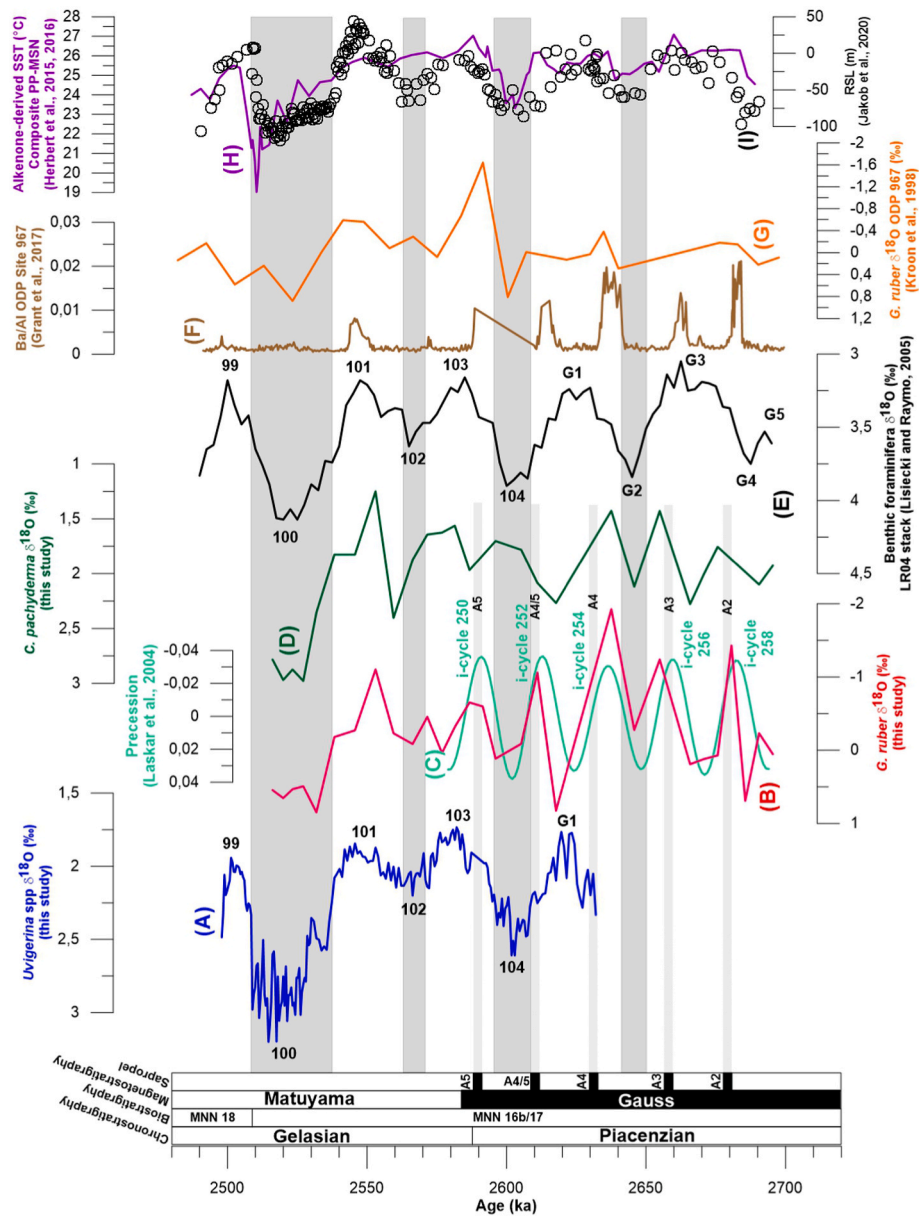
Fig. 2. The multi-species δ^{18}O record reconstructed for this work presented in time, according to our age model, and its correlation to other significant records. Left: essential chronostratigraphic information on the studied record, with indication of sapropel position. (A) High-resolution δ^{18}O record for *Uvigerina* spp (blue). (B) δ^{18}O record for *G. ruber* (red) compared to (C) the precession curve (sea green) of Laskar et al. (2004). (D) δ^{18}O record for *C. pachyderma* (dark green). (E) The LR04 benthic δ^{18}O stack (black) of Lisiecki and Raymo (2005). (F) The Ba/Al ratio measured at ODP Site 967 (brown) by Grant et al. (2017). (G) The δ^{18}O record for *G. ruber* at ODP 967 site (orange) by Kroon et al. (1998). (H) The composite PP-MSN Alkenone-derived Mediterranean SST record (purple) of Herbert et al., (2015), 2016; PP = Punta Piccola, MSN = Monte San Nicola. (I) The relative sea level (RSL) curve for the North Atlantic (open circles) by Jakob et al. (2020). All isotope data are reported in per mil (‰) relative to the VPDB standard. The thicker gray bands indicate glacial periods (MIS G2, 104, 102, 100), while the thinner ones highlight the cluster A sapropels occurrences (A5, A4/5, A4, A3, A2).

4. Results and discussion

4.1. Oxygen isotope stratigraphy and chronology

In our multi-species δ^{18}O record, the major isotopic events known to occur in the interval ~2.7–2.5 Ma are unambiguously depicted (Fig. 2). In particular, the high-resolution record of *Uvigerina* spp clearly delineates the obliquity-driven δ^{18}O oscillations between MIS G1 and MIS 99, as reported by Lisiecki and Raymo (2005). Both the "Nicola bed" (sapropel A5: 0.25 – 0 m) and the Gauss/Matuyama geomagnetic reversal, as defined by Capraro et al. (2022) at +0.3 m, fall unequivocally in the lower part of full MIS 103 (Fig. 2), in agreement with the Mediterranean deep-sea and open ocean records (Emeis et al., 2000;

Grant et al., 2017; Laj and Channell, 2007, 2015; Lourens et al., 1996).

The age model was assessed by linear interpolation among 9 tie-points (Table 1) identified as distinctive peaks in the δ^{18}O stratigraphy and/or sapropel layers. The LR04 benthic stack (Lisiecki and Raymo, 2005) was employed as target curve in defining the ages for MIS 99, 100, 102 and 104. Ages for sapropel layers A5, A4/5, A4, A3 and A2 were imported from astronomically calibrated eastern Mediterranean deep-sea records (Emeis et al., 2000; Lourens et al., 1996). Alignment of our multi-species δ^{18}O record to the LR04 benthic stack, as well as the position of sapropel layers, is shown in Fig. 2. In the studied segment, sediment accumulation rates oscillate on average around 7 cm/kyr, in general agreement with previous estimates obtained for the lower part of the Mandorlo section (Capraro et al., 2022) and other central

Table 1
Main chronostratigraphic tie-points (MIS and MPRS) employed to assess the age-depth plot reported in Fig. 3, together with estimated sediment accumulation rates, resolution in kyrs (per 5 cm) and references, respectively. Our tuning error is comparable to the uncertainty of LR04 stack (adopted target curve for the tuning) which was estimated to be 0.006 Ma for the time interval between 3 and 1 Ma (Lisiecki and Raymo, 2005).

Tie-point	Level (cm)	Age (ka)	Sed. rate (cm/kyr)	Resolution in kyr (x 5 cm)	References
MIS 99	600	2507.5			LR04 benthic stack (Lisiecki and Raymo, 2005)
			10.4	0.479	
MIS 100	365	2530			LR04 benthic stack (Lisiecki and Raymo, 2005)
			5.4	0.921	
MIS 102	175	2565			LR04 benthic stack (Lisiecki and Raymo, 2005)
			7.6	0.657	
Nicola bed (A5) *(midst MIS 103)*	0	2588			(Emeis et al., 2000; Lourens et al., 1996)
			8.7	0.574	
MIS 104	−170	2607.5			LR04 benthic stack (Lisiecki and Raymo, 2005)
			5.7	0.875	
A4/5 *(end MIS G1)*	−190	2611			(Emeis et al., 2000; Lourens et al., 1996)
			5.2	0.955	
A4 *(onset MIS G1)*	−300	2632			(Emeis et al., 2000; Lourens et al., 1996)
			5.5	0.912	
A3 *(end MIS G3)*	−442.5	2658			(Emeis et al., 2000; Lourens et al., 1996)
			8.1	0.618	
A2 *(onset MIS G3)*	−612.5	2679			(Emeis et al., 2000; Lourens et al., 1996)

Fig. 3. Age-depth plot based on the major chronostratigraphic events recognized in the lower part of the Mandorlo section. The orthogonal polynomial regression line equation and the R-squared coefficient are explicitly reported. Corresponding ages and levels in the local stratigraphy are reported in Table 1.

Equation Y = 2585.7144 - 0.1446716 * X + 1.8710528e-05 * pow(X,2)
Number of data points used = 9
Coefficient of determination, R-squared = 0.9960230

Mediterranean deep-sea successions (Capraro et al., 2011; Incarbona et al., 2009; Toucanne et al., 2012) (Table 1). The depth/age plot shows a $R^2 = 0.996$ value for the polynomial best fit (Fig. 3).

MIS 100 was a period of massive ice accumulation rates in the Northern Hemisphere and severe decrease in the global (eustatic) sea level (Jakob et al., 2020; Rohling et al., 2014) (Fig. 2). According to the paleotemperature reconstructions of Herbert et al. (2016, 2015) for the Monte San Nicola – Punta Piccola composite section, the MIS 100 glaciation caused a ~4 °C decrease in the central Mediterranean SSTs (i. e., from ~23 °C in MIS 104 to ~19 °C in MIS 100). In the Mandorlo section, in agreement with most $\delta^{18}O$ records globally (Lisiecki and Raymo, 2005), MIS 100 provides a sharp isotopic signature as it includes the highest $\delta^{18}O$ values of the whole study record for both *C. pachyderma*, *G. ruber* and *Uvigerina* spp (Fig. 2). The MIS 100 interval contains the Top of *D. pentaradiatus*, arguably the most reliable and convenient biohorizon for approximating the base of the Gelasian Stage (Channell et al., 1992; Rio et al., 1998), that in the Mandorlo section was constrained by Capraro et al. (2022) at ~4.6 m above the Nicola bed (Fig. 2), with an estimated age of ~2.512 Ma, in line with previous astronomical estimates obtained in Sicily and the eastern Mediterranean (Hilgen, 1991; Lourens et al., 1996; Raffi et al., 2006; Sprovieri et al.,
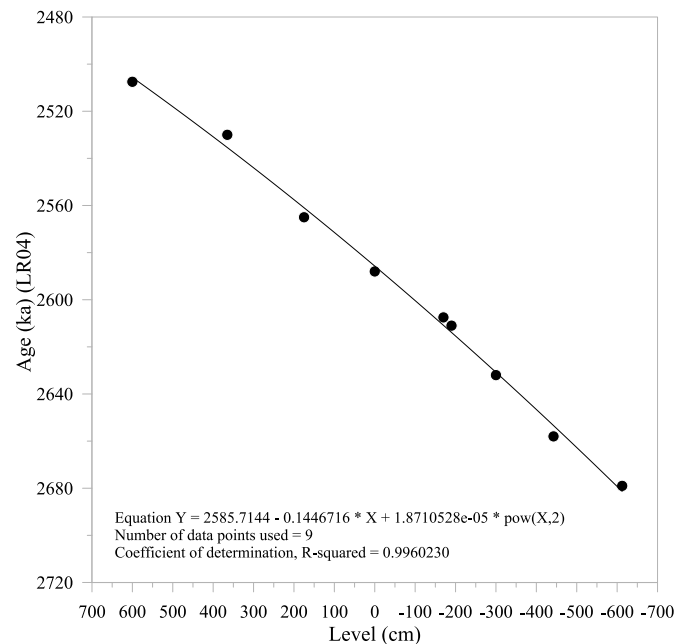
1998). Data presented in this paper allowed establishing a new interpolated age for the Gauss/Matuyama reversal (as defined in Capraro et al., 2022) of 2.585 ± 0.006 Ma, consistent with the widely accepted 2.581–2.587 Ma estimates (Cande and Kent, 1995; Lourens et al., 1996; Ohno et al., 2012).

All the Mediterranean Precession-Related Sapropel layers (MPRS) of cluster A fall as expected in our benthic isotope stratigraphy, with the exception of sapropel A1 that was not considered in Capraro et al. (2022) (Fig. 2). Namely, A2 and A3 occur at the onset and the end of MIS G3 respectively, A4 and A4/5 at the onset and end of MIS G1 respectively, A5 (the "Nicola bed") in MIS 103. Individual sapropel layers correspond to low $\delta^{18}O$ values of the surface-dwelling *G. ruber*, pointing to conditions of strong stratification of the water column with warm, low-salinity waters atop (Kroon et al., 1998). These conditions are in keeping with the well-established scenario of increased monsoon-related freshwater runoff from the coasts of North Africa during periods of insolation maxima (i.e., precession minima) and sapropel deposition in the eastern Mediterranean (Amies et al., 2019; Rohling et al., 2002, 2004a,b, 2015). Consequently, the two records oscillate out of phase in correspondence to the sapropel layers of cluster A, when the precession-related climate forcing over the Mediterranean intensified and eventually took over the background glacioeustatic (obliquity-driven) signal (Fig. 2). However, the mismatch of *G. ruber* and *Uvigerina* spp $\delta^{18}O$ curves may be an artefact due to different resolution and in any case may reflect the different habitats of the two species, respectively dependent on the evaporation *versus* runoff and precipitation balance and on deepwater and seafloor dynamics (Di Donato et al., 2022; Incarbona and Sprovieri, 2020; Rohling et al., 2004a,b).

4.2. Suborbital climate variability

Becker et al. (2005) analyzed the fine-scale anatomy of the stratigraphic interval between MIS 101 and MIS 99 in a profile adjacent to the Mandorlo section, to discover that the MIS 100 glacial was characterized by a pervasive suborbital climatic variability (in the 4–8 kyr time domain) in the benthic $\delta^{18}O$ record. We have broadened the investigation to the interval between the MIS G2/MIS G1 transition and the

uppermost part of MIS 99 with a resolution of one sample every 5 cm (i. e., ~750 yr on average), slightly looser than that attained by Becker et al. (2005) (i.e. one sample every 3 cm, that is ~430 yr average) but still adequate to unveil the possible presence of suborbital signals within. Evidence of a strong short-term variability was found across a large part of our *Uvigerina* spp δ^{18}O record (Fig. 4A). Spectral analysis indicates that such oscillations abide to a 4–6 kyr periodicity, significant at the 95% confidence level (Fig. 5A). Wavelet analysis (Fig. 5B) confirms that this signal is strong throughout the 2540-2500 ka (MIS 100) interval, but also from 2630 to 2590 ka (MIS G1 – MIS 104).

By analogy with the interpretations proposed to explain the high-frequency climatic fluctuations found in the late Pleistocene and Holocene (i.e., the Dangsaard-Oeschger and Bond cycles; Cacho et al., 2000; Moreno et al., 2005), one may speculate that the millennial-scale oscillations found in the Mandorlo section might have been driven by the dynamics of the Atlantic Ocean. Indeed, a tight relationship is believed to have occurred between the changes in the strength of the Atlantic Meridional Overturning Circulation (AMOC) and the short-term climate variability in the Mediterranean across the last glacial cycles (Cacho et al., 2000; Moreno et al., 2005; Sprovieri et al., 2012), according to mechanisms that may also be inferred for the MIS 100 and MIS 104 glacials. Our data show that millennial scale variability is a pervasive characteristic of our record and a ~5 kyr-periodicity is also manifest within interglacial MIS G1 (Fig. 4B–5B). Interglacial climate instability at the suborbital scale is well documented for the Holocene and MIS 5 (Incarbona et al., 2008; Martrat et al., 2014; Mayewski et al., 2004; Oppo et al., 2001; Sprovieri et al., 2006; Tzedakis et al., 2018), and recently the relative sea-level reconstruction of Jakob et al. (2020) for

the North Atlantic provides evidence of a strong high-frequency interglacial variability across the Piacenzian-Gelasian transition as well (Fig. 4D). Regarding another possible origin of the 5 kyr cycle at Monte San Nicola, wavelet analyses (Fig. 5) indicate that the strength of the suborbital signal varies in phase with the ca. 20-kyr precessional cyclicity (peaks ~2630 ka, i.e. i-cycle 254, A4, G2/G1 transition; at ~2600 ka, i.e. i-cycle 252, A4/5, MIS 104; at ~2530, i.e. onset MIS 100 and at ~2510 ka, i.e. end MIS 100 2530, 2600, and 2630 ka), thus suggesting that the observed millennial-scale climate variability during the time interval analyzed in this study may primarily respond to low-latitude processes. Regardless, the underlying mechanism for the strong suborbital signal found within our record remain ambiguous in the lack of independent auxiliary data, and this topic falls beyond the scope of this paper.

5. Conclusions

The planktonic and benthic foraminifera δ^{18}O and δ^{13}C records reconstructed for the Mandorlo section across the Piacenzian/Gelasian boundary unraveled a long-term, obliquity-driven glacial-interglacial variability that is fully consistent with the open ocean records globally. Superimposed is a high-frequency cyclicity in the ca. 5-kyr time domain, which is especially manifest during two (MIS 104 and MIS 100) of the three glacial periods found within our study interval. Yet, interglacial MIS G1 and glacial MIS 104 contains evidence of a fully comparable suborbital cyclicity, the origin of which remain ambiguous. Although we speculate that the dynamics of Atlantic Ocean and/or the orbital precession may play a critical role in this regard, further studies
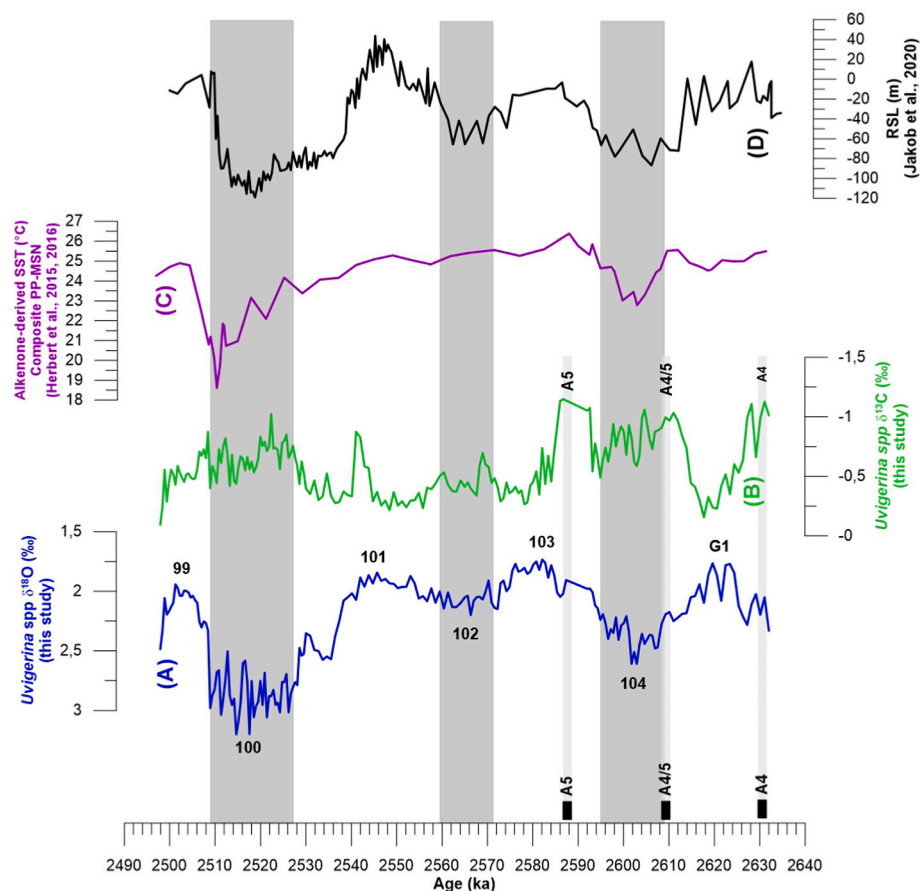

Fig. 4. (A), (B) The high-resolution δ^{18}O (blue) and δ^{13}C (light green) records for *Uvigerina* spp, respectively, compared to other crucial Mediterranean and open ocean records. On the bottom: chronology of the studied record and indication of glacial/interglacial periods (MISs). (C) The Alkenone-derived Mediterranean SST reconstruction (purple curve) of Herbert et al. (2015, 2016). (D) The relative sea level (RSL) curve for the North Atlantic (black) by Jakob et al. (2020). The thicker gray bands highlight glacial periods (MIS 104, 102 and 100) while the thinner gray bands point out the sapropels occurrences (A5, A4/5 and A4).
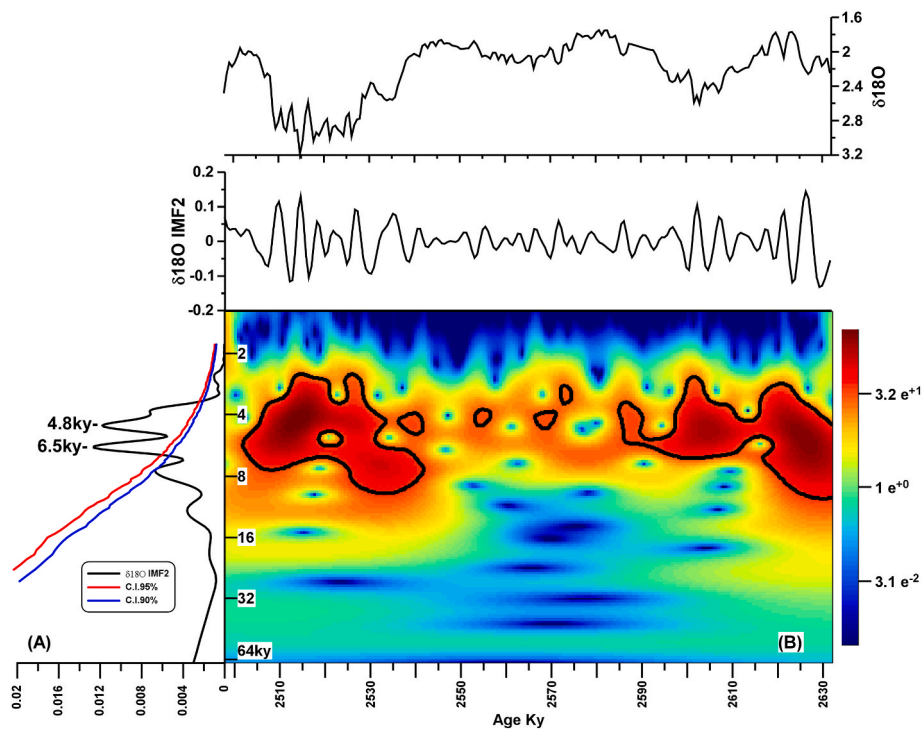
Fig. 5. (A) Spectral analysis of the IMF2 component for the δ¹⁸O record of *Uvigerina* spp, unraveling the presence of a suborbital periodicity in the 4–6 kyr time domain. (B) Wavelet analysis confirming its pervasive occurrence throughout the MIS G1- MIS104 interval (~2630–2590 ka) and MIS 100 (raw version is displayed on top).

will be needed to shed new light on the issue.

On top of these results, we also confirmed and refined the chronology of the bio-magnetostratigraphic events identified by Capraro et al. (2022) around the Piacenzian/Gelasian boundary. Specifically, for the very first time in the Monte San Nicola section it is demonstrated that both the "Nicola bed" (sapropel A5) and the Gauss/Matuyama geomagnetic reversal occur in the midst of interglacial MIS 103, in keeping with open-ocean reference records. These results both confirm the reliability of this succession as the type-area for the Gelasian GSSP and emphasize its aptness to serve as a reference for high-resolution paleoclimatic and paleoceanographic studies in the upper Piacenzian to lower Calabrian interval.

Authors contributions

Each author has played a fundamental role for the development of this manuscript. Specifically: E.Z.: samples collection, data production, writing; S.B., A.I.: conceptualization, data curation, writing; A.D.S., P.F., E.F., S.G., P.M., I.R., N.S., F.S., M.S.: samples analysis, data production and validation; S.D., E.D.S., R.S. and D.R.:guidance and assistance in the field; L.C.: supervision, samples collection, writing.

Declaration of competing interest

The authors declare that they have no known competing financial interests or personal relationships that could have appeared to influence the work reported in this paper.

Data availability

Data will be made available on request.

Acknowledgments

We are grateful to G. Zanchetta, Editor of QSR, and two anonymous

References

Amies, J.D., Rohling, E.J., Grant, K.M., Rodríguez-Sanz, L., Marino, G., 2019. Quantification of African monsoon runoff during last interglacial sapropel S5. Paleoceanogr. Paleoclimatol. 34, 1487–1516. https://doi.org/10.1029/2019PA003652.

Bartoli, G., Sarnthein, M., Weinelt, M., Erlenkeuser, H., Garbe-Schonberg, D., Lea, D., 2005. Final closure of Panama and the onset of northern hemisphere glaciation. Earth Planet Sci. Lett. 237, 33–44. https://doi.org/10.1016/j.epsl.2005.06.020.

Becker, J., Lourens, L., Hilgen, F., van der Laan, E., Kouwenhoven, T., Reichart, G., 2005. Late pliocene climate variability on Milankovitch to millennial time scales: a high-resolution study of MIS100 from the Mediterranean. Palaeogeogr. Palaeoclimatol. Palaeoecol. https://doi.org/10.1016/j.palaeo.2005.06.020.

Bunn, A.G., 2010. Statistical and visual crossdating in R using the dplR library. Dendrochronologia. https://doi.org/10.1016/j.dendro.2009.12.001.

Cacho, I., Grimalt, J.O., Sierro, F.J., Shackleton, N., Canals, M., 2000. Evidence for enhanced Mediterranean thermohaline circulation during rapid climatic coolings. Earth Planet Sci. Lett. 183, 417–429. https://doi.org/10.1016/S0012-821X(00)00296-X.

Cande, S.C., Kent, D.V., 1995. Revised calibration of the geomagnetic polarity timescale for the Late Cretaceous and Cenozoic. J. Geophys. Res. Solid Earth 100, 6093–6095. https://doi.org/10.1029/94JB03098.

Capraro, L., Bonomo, S., Di Stefano, A., Ferretti, P., Fornaciari, E., Galeotti, S., Incarbona, A., Macrì, P., Raffi, I., Sabatino, N., Speranza, F., Sprovieri, M., Stefano, E.D., Sprovieri, R., Rio, D., 2022. The Monte san Nicola section (Sicily) revisited: a potential unit-stratotype of the Gelasian stage. Quat. Sci. Rev. 278, 107367 https://doi.org/10.1016/j.quascirev.2021.107367.

Capraro, L., Massari, F., Rio, D., Fornaciari, E., Backman, J., Channell, J.E.T., Macrì, P., Prosser, G., Speranza, F., 2011. Chronology of the lower–Middle Pleistocene succession of the south-western part of the Crotone basin (Calabria, southern Italy). Quat. Sci. Rev. 30, 1185–1200. https://doi.org/10.1016/j.quascirev.2011.02.008.

Channell, J., Di Stefano, E., Sprovieri, R., 1992. Calcareous plankton biostratigraphy, magnetostratigraphy and paleoclimatic history of the Plio-Pleistocene Monte San Nicola section (southern Sicily). Boll. Soc. Paleontol. Ital. 31, 351–382.

Di Donato, V., Sgarrella, F., Sprovieri, R., Di Stefano, E., Martín-Fernández, J.A., Incarbona, A., 2022. High-frequency modification of the central Mediterranean seafloor environment over the last 74 ka. Palaeogeogr. Palaeoclimatol. Palaeoecol. 593, 110924 https://doi.org/10.1016/j.palaeo.2022.110924.

Emeis, K.-C., Sakamoto, T., Wehausen, R., Brumsack, H.-J., 2000. The sapropel record of the eastern Mediterranean sea — results of ocean Drilling program Leg 160. Palaeogeogr. Palaeoclimatol. Palaeoecol. 158, 371–395. https://doi.org/10.1016/S0031-0182(00)00059-6.

Gibbard, P.L., Head, M.J., Walker, M.J.C., 2010. Formal ratification of the Quaternary System/period and the Pleistocene series/Epoch with a base at 2.58 Ma. J. Quat. Sci. 25, 96–102. https://doi.org/10.1002/jqs.1338.

Grant, K.M., Rohling, E.J., Westerhold, T., Zabel, M., Heslop, D., Konijnendijk, T., Lourens, L., 2017. A 3 million year index for North African humidity/aridity and the implication of potential pan-African Humid periods. Quat. Sci. Rev. 171, 100–118. https://doi.org/10.1016/j.quascirev.2017.07.005.

Hayashi, T., Yamanaka, T., Hikasa, Y., Sato, M., Kuwahara, Y., Ohno, M., 2020a. Latest Pliocene Northern Hemisphere glaciation amplified by intensified Atlantic meridional overturning circulation. Commun. Earth Environ. 1 https://doi.org/10.1038/s43247-020-00023-4.

Hayashi, T., Yamanaka, T., Hikasa, Y., Sato, M., Kuwahara, Y., Ohno, M., 2020b. Latest Pliocene Northern Hemisphere glaciation amplified by intensified Atlantic meridional overturning circulation. Commun. Earth Environ. 1, 25. https://doi.org/10.1038/s43247-020-00023-4.

Head, M.J., Pillans, B., Zalasiewicz, J.A., the ICS Subcommission on Quaternary Stratigraphy, 2021. Formal ratification of subseries for the Pleistocene Series of the Quaternary System. Int. Union Geol. Sci. 44, 241–247. https://doi.org/10.18814/epiiugs/2020/020084.

Herbert, T.D., Lawrence, K.T., Tzanova, A., Peterson, L.C., Caballero-Gill, R., Kelly, C.S., 2016. Late Miocene global cooling and the rise of modern ecosystems. Nat. Geosci. https://doi.org/10.1038/ngeo2813.

Herbert, T.D., Ng, G., Cleaveland Peterson, L., 2015. Evolution of Mediterranean sea surface temperatures 3.5-1.5 Ma: regional and hemispheric influences. Earth Planet Sci. Lett. https://doi.org/10.1016/j.epsl.2014.10.006.

Hilgen, F.J., 1991. Astronomical calibration of Gauss to Matuyama sapropels in the Mediterranean and implication for the geomagnetic polarity time scale. Earth Planet Sci. Lett. https://doi.org/10.1016/0012-821X(91)90206-W.

Huang, N., Shen, Z., Long, S., Wu, M., Shih, H., Zheng, Q., Yen, N., Tung, C., Liu, H., 1998. The empirical mode decomposition and the Hilbert spectrum for nonlinear and non-stationary time series analysis. Proc. R. Soc. -Math. Phys. Eng. Sci. 454, 903–995. https://doi.org/10.1098/rspa.1998.0193.

Incarbona, A., Sprovieri, M., 2020. The Postglacial isotopic record of Intermediate water Connects Mediterranean sapropels and organic-rich layers. Paleoceanogr. Paleoclimatol. 35 (10), e2020PA004009 https://doi.org/10.1029/2020PA004009.

Incarbona, A., Stefano, E.D., Bonomo, S., 2009. Calcareous nannofossil biostratigraphy of the central Mediterranean Basin during the last 430,000 years. Stratigraphy. https://doi.org/10.2307/1484315.

Incarbona, A., Di Stefano, E., Patti, B., Pelosi, N., Bonomo, S., Mazzola, S., Sprovieri, R., Tranchida, G., Zgozi, S., Bonanno, A., 2008. Holocene millennial-scale productivity variations in the Sicily channel (Mediterranean sea). Paleoceanography 23. https://doi.org/10.1029/2007PA001581.

Jakob, K.A., Wilson, P.A., Pross, J., Ezard, T.H.G., Fiebig, J., Repschläger, J., Friedrich, O., 2020. A new sea-level record for the Neogene/Quaternary boundary reveals transition to a more stable East Antarctic Ice Sheet. Proc. Natl. Acad. Sci. 117, 30980–30987. https://doi.org/10.1073/pnas.2004209117.

Kroon, D., Alexander, I., Little, M., Lourens, L.J., Matthewson, A., Robertson, A.H.F., Sakamoto, T., 1998. Oxygen isotope and Sapropel stratigraphy in the eastern Mediterranean during the last 3.2 million years. Proc. Ocean Drill. Progr. Sci. Results. https://doi.org/10.2973/odp.proc.sr.160.071.1998.

Laj, C., Channell, J.E.T., 2015. Geomagnetic excursions. In: Treatise Geophys, Second. https://doi.org/10.1016/B978-0-444-53802-4.00104-4.

Laj, C., Channell, J.E.T., 2007. Geomagnetic excursions. In: Schubert, G. (Ed.), Geomagnetism, pp. 373–416. https://doi.org/10.1016/B978-044452748-6.00095-X.

Laskar, J., Robutel, P., Joutel, F., Gastineau, M., Correia, A.C.M., Levrard, B., 2004. A long-term numerical solution for the insolation quantities of the Earth. Astronomy Astrophys. 428, 261–285.

Lisiecki, L.E., Raymo, M.E., 2005. A Pliocene-Pleistocene stack of 57 globally distributed benthic δ18O records. Paleoceanography 20. https://doi.org/10.1029/2004PA001071.

Liu, Y., Liang, X.S., Weisberg, R.H., 2007. Rectification of the bias in the wavelet power spectrum. J. Atmos. Ocean. Technol. https://doi.org/10.1175/2007JTECHO511.1.

Lourens, L.J., Antonarakou, A., Hilgen, F.J., Van Hoof, A.A.M., Vergnaud-Grazzini, C., Zachariasse, W.J., 1996. Evaluation of the Plio-Pleistocene astronomical timescale. Paleoceanography 11, 391–413. https://doi.org/10.1029/96PA01125.

Luukko, P.J.J., Helske, J., Rasanen, E., 2016. Introducing libeemd: a program package for performing the ensemble empirical mode decomposition. Comput. Stat. 31, 545–557. https://doi.org/10.1007/s00180-015-0603-9.

Martrat, B., Jimenez-Amat, P., Zahn, R., Grimalt, J.O., 2014. Similarities and dissimilarities between the last two deglaciations and interglaciations in the North Atlantic region. Quat. Sci. Rev. 99, 122–134. https://doi.org/10.1016/j.quascirev.2014.06.016.

Mayewski, P.A., Rohling, E.E., Curt Stager, J., Karlén, W., Maasch, K.A., Meeker, L.D., Meyerson, E.A., Gasse, F., van Kreveld, S., Holmgren, K., al, et al., 2004. Holocene climate variability. Quat. Res. 62, 243–255. https://doi.org/10.1016/j.yqres.2004.07.001.

McClymont, E.L., Ford, H.L., Ho, S.L., Tindall, J.C., Haywood, A.M., Alonso-Garcia, M., Bailey, I., Berke, M.A., Littler, K., Patterson, M.O., Petrick, B., Peterse, F., Ravelo, A. C., Risebrobakken, B., De Schepper, S., Swann, G.E.A., Thirumalai, K., Tierney, J.E., van der Weijst, C., White, S., Abe-Ouchi, A., Baatsen, M.L.J., Brady, E.C., Chan, W.-L., Chandan, D., Feng, R., Guo, C., von der Heydt, A.S., Hunter, S., Li, X.,

Lohmann, G., Nisancioglu, K.H., Otto-Bliesner, B.L., Peltier, W.R., Stepanek, C., Zhang, Z., 2020. Lessons from a high CO₂ world: an ocean view from ∼ 3 million years ago. Clim. Past 16, 1599–1615. https://doi.org/10.5194/cp-16-1599-2020.

Moreno, A., Cacho, I., Canals, M., Grimalt, J.O., Sánchez-Goñi, M.F., Shackleton, N., Sierro, F.J., 2005. Links between marine and atmospheric processes oscillating on a millennial time-scale. A multi-proxy study of the last 50,000yr from the Alboran Sea (Western Mediterranean Sea). Quat. Sci. Rev. 24, 1623–1636. https://doi.org/10.1016/j.quascirev.2004.06.018.

Ohno, M., Hayashi, T., Komatsu, F., Murakami, F., Zhao, M., Guyodo, Y., Acton, G., Evans, H.F., Kanamatsu, T., 2012. A detailed paleomagnetic record between 2.1 and 2.75 Ma at IODP site U1314 in the North Atlantic: geomagnetic excursions and the Gauss-Matuyama transition. Geochem. Geophys. Geosystems 13. https://doi.org/10.1029/2012GC004080.

Oppo, D.W., Keigwin, L.D., McManus, J.F., Cullen, J.L., 2001. Persistent suborbital climate variability in marine isotope stage 5 and termination II. Paleoceanography 16, 280–292. https://doi.org/10.1029/2000PA000527.

Pasini, G., Colalongo, M.L., 1997. The pliocene–Pleistocene boundary-stratotype at Vrica, Italy. In: Van Couvering, J.A. (Ed.), The Pleistocene Boundary and the Beginning of the Quaternary. Cambridge University Press, pp. 15–45.

Raffi, I., Backman, J., Fornaciari, E., Pälike, H., Rio, D., Lourens, L., Hilgen, F., 2006. A review of calcareous nannofossil astrobiochronology encompassing the past 25 million years. Quat. Sci. Rev. 25, 3113–3137. https://doi.org/10.1016/j.quascirev.2006.07.007.

Rio, D., Sprovieri, R., Di Stefano, E., 1994. The Gelasian Stage: a proposal of a new chronostratigraphic unit of the Pliocene series. Rev. Ital. Palaeontol. E Stratigr.

Rio, R. Sprovieri, Castradori, D., Di Stefano, E., 1998. The Gelasian Stage (Upper Pliocene): a new unit of the global standard chronostratigraphic scale. Int. Union Geol. Sci. 21, 82–87. https://doi.org/10.18814/epiiugs/1998/v21i2/002.

Rohling, E.J., Cane, T.R., Cooke, S., Sprovieri, M., Bouloubassi, I., Emeis, K.C., Schiebel, R., Kroon, D., Jorissen, F.J., Lorre, A., Kemp, A.E.S., 2002. African monsoon variability during the previous interglacial maximum. Earth Planet Sci. Lett. 202, 61–75. https://doi.org/10.1016/S0012-821X(02)00775-6.

Rohling, E.J., Marsh, R., Wells, N.C., Siddall, M., Edwards, N.R., 2004a. Similar meltwater contributions to glacial sea level changes from Antarctic and northern ice sheets. Nature 430, 1016–1021. https://doi.org/10.1038/nature02859.

Rohling, E.J., Sprovieri, M., Cane, T., Casford, J.S.L., Cooke, S., Bouloubassi, I., Emeis, K. C., Schiebel, R., Rogerson, M., Hayes, a., Jorissen, F.J., Kroon, D., 2004b. Reconstructing past planktic foraminiferal habitats using stable isotope data: a case history for Mediterranean sapropel S5. Mar. Micropaleontol. 50 (1–2), 89–123. https://doi.org/10.1016/S0377-8398(03)00068-9.

Rohling, E.J., Foster, G.L., Grant, K.M., Marino, G., Roberts, A.P., Tamisiea, M.E., Williams, F., 2014. Sea-level and deep-sea-temperature variability over the past 5.3 million years. Nature 508, 477–482. https://doi.org/10.1038/nature13230.

Rohling, E.J., Marino, G., Grant, K.M., 2015. Mediterranean climate and oceanography, and the periodic development of anoxic events (sapropels). Earth Sci. Rev. 143, 62–97. https://doi.org/10.1016/j.earscirev.2015.01.008.

Seki, O., Foster, G.L., Schmidt, D.N., Mackensen, A., Kawamura, K., Pancost, R.D., 2010. Alkenone and boron-based Pliocene pCO₂ records. Earth Planet Sci. Lett. 292, 201–211. https://doi.org/10.1016/j.epsl.2010.01.037.

Shackleton, N.J., Backman, J., Zimmerman, H., Kent, D.V., Hall, M.A., Roberts, D.G., Schnitker, D., Baldauf, J.G., Desprairies, A., Homrighausen, R., Huddlestun, P., Keene, J.B., Kaltenback, A.J., Krumsiek, K.A.O., Morton, A.C., Murray, J.W., Westbrg-Smith, J., 1984. Oxygen isotope calibration of the onset of ice-rafting and history of glaciation in the North Atlantic region. Nature 307, 620–623. https://doi.org/10.1038/307620a0.

Shackleton, N.J., Hall, M.A., Pate, D., 1995. Pliocene stable isotope stratigraphy of site 846. Proc. Ocean Drill. Progr. Sci. Results 138.

Spötl, C., Vennemann, T.W., 2003. Continuous-flow isotope ratio mass spectrometric analysis of carbonate minerals. Rapid Commun. Mass Spectrom. 17, 1004–1006. https://doi.org/10.1002/rcm.1010.

Sprovieri, M., Stefano, E.D., Incarbona, A., Manta, D.S., Pelosi, N., d'Alcalà, M.R., Sprovieri, R., 2012. Centennial- to millennial-scale climate oscillations in the Central-Eastern Mediterranean Sea between 20,000 and 70,000 years ago: evidence from a high-resolution geochemical and micropaleontological record. Quat. Sci. Rev. 46, 126–135. https://doi.org/10.1016/j.quascirev.2012.05.005.

Sprovieri, R., Di Stefano, E., Howell, M., Sakamoto, T., Di Stefano, A., Marino, M., 1998. Integrated calcareous plankton biostratigraphy and cyclostratigraphy at Site 964. Proc. Ocean Drill. Progr. Sci. Results.

Sprovieri, R., Stefano, E.D., Incarbona, A., Oppo, D.W., 2006. Suborbital climate variability during Marine Isotopic Stage 5 in the central Mediterranean basin: evidence from calcareous plankton record. Quat. Sci. Rev. 25, 2332–2342. https://doi.org/10.1016/j.quascirev.2006.01.035.

Toucanne, S., Jouet, G., Ducassou, E., Bassetti, M.-A., Dennielou, B., Minto'o, C.M.A., Lahmi, M., Touyet, N., Charlier, K., Lericolais, G., Mulder, T., 2012. A 130,000-year record of Levantine Intermediate water flow variability in the Corsica trough, western Mediterranean sea. Quat. Sci. Rev. 33, 55–73. https://doi.org/10.1016/j.quascirev.2011.11.020.

Tzedakis, P.C., Drysdale, R.N., Margari, V., Skinner, L.C., Menviel, L., Rhodes, R.H., Taschetto, A.S., Hodell, D.A., Crowhurst, S.J., Hellstrom, J.C., Fallick, A.E., Grimalt, J.O., McManus, J.F., Martrat, B., Mokeddem, Z., Parrenin, F., Regattieri, E., Roe, K., Zanchetta, G., 2018. Enhanced climate instability in the North Atlantic and southern Europe during the last interglacial. Nat. Commun. 9, 4235. https://doi.org/10.1038/s41467-018-06683-3.

Verhallen, P.J.J.M., 1987. Early development of Bulimina marginata in relation to paleoenvironmental changes in the Mediterranean. Proc. K. Akad. Voor Wet.

Westerhold, T., Marwan, N., Drury, A.J., Liebrand, D., Agnini, C., Anagnostou, E., Barnet, J.S.K., Bohaty, S.M., De Vleeschouwer, D., Florindo, F., Frederichs, T., Hodell, D.A., Holbourn, A.E., Kroon, D., Lauretano, V., Littler, K., Lourens, L.J., Lyle, M., Pälike, H., Röhl, U., Tian, J., Wilkens, R.H., Wilson, P.A., Zachos, J.C., 2020. An astronomically dated record of Earth's climate and its predictability over the last 66 million years. Science. https://doi.org/10.1126/science.aba6853.

Wu, Z., Huang, N.E., 2009. Ensemble empirical mode decomposition: a noise-assisted data analysis method. Adv. Adapt. Data Anal. 1, 1–41. https://doi.org/10.1142/s1793536909000047.

Zijderveld, J., Hilgen, F., Langereis, C., Verhallen, P., Zachariasse, W., 1991. Integrated magnetostratigraphy and biostratigraphy of the upper pliocene-lower Pleistocene from the Monte Singa and Crotone areas in Calabria, Italy. Earth Planet Sci. Lett. 107.